American Mineralogist, Volume 73, pages 692–700, 1988

Sapphirine granulites from the Kakanuru area, Eastern Ghats, India

D. C. KAMINENI*
Geological Survey of Canada, 601 Booth Street, Ottawa K1A 0E8, Canada
A. T. RAO
Department of Geology, Andhra University, Waltair, India 530003

ABSTRACT

Sapphirine in the granulitic terrane of the Eastern Ghats, near Kakanuru, India, has three modes of occurrence: (1) as a dominant mineral in a rock of possible regolithic origin, (2) generally as rims around spinel and magnetite in khondalite, and (3) replacing spinel in pyroxenites. All three types have distinct compositional characteristics; the X_{Mg} [$Mg/(Mg + Fe^{2+})$] value increases from 0.770 to 0.964 from type 1 to type 3. The parageneses of various types are discussed.

Temperature and pressure estimates based on suitable mineral pairs and calibrated geothermometers and geobarometers indicate extremely high grade metamorphic conditions. The temperature estimate, based on two-pyroxene and two-feldspar geothermometers, ranges from 840 to 1050 °C. The estimated pressure is about 7.3 kbar. These P-T conditions are in accordance with the sapphirine paragenesis. The temperature estimate from the garnet-biotite geothermometer yields a lower value (≃600 °C) that can be attributed to a subsequent metamorphic event accompanied by hydration and metasomatism.

INTRODUCTION

Sapphirine-bearing granulites are very useful in deducing the metamorphic conditions of the lower crust. This is mainly because sapphirine extends over a wide range of pressure-temperature (P-T) conditions, as documented in experimental and theoretical investigations (Newton, 1972; Seifert, 1974; Ackermand et al., 1975; Bishop and Newton, 1975; Hensen, 1986, 1987). The occurrence of sapphirine-bearing rocks has been noted in the Eastern Ghats granulite terrane by many workers (see Grew, 1982). The Eastern Ghats granulite belt, oriented NE–SW along the east coast of India (Fig. 1), forms prominent hill ranges and is mainly composed of khondalites and charnockites. The khondalites comprise a variety of metamorphic rocks of sedimentary protoliths, quartz + orthoclase + garnet + sillimanite ± graphite being the most common assemblage. The charnockites, containing garnet + pyroxene–bearing assemblages, show a wide spectrum of lithology ranging from felsic to mafic end members. In the eastern part of the belt, the charnockites are structurally emplaced into khondalites along axial regions of the folds, whereas in the western margin, they occur along thrust sheets.

In this paper, petrographic characteristics, bulk rock composition, mineral chemistry, and metamorphic conditions of sapphirine-bearing assemblages from the Kakanuru area are described. The region is covered by thick tropical forest and is in close proximity to the western margin of the Eastern Ghats. Geographically, the region falls in parts of the East Godavari and Visakhapatnam districts of Andhra Pradesh.

GENERAL GEOLOGY OF THE AREA

A brief account of the geology around Kakanuru, based on the preliminary map of Singh and Augustine (1978), is depicted in Figure 1. The area is essentially composed of three broad units: (1) khondalite, (2) charnockite, and (3) amphibolite. Khondalite is the most abundant map unit containing the assemblage quartz + feldspars + garnet + sillimanite ± sapphirine ± spinel. On some outcrops, this unit displays extreme alteration, due to tropical weathering, developing laterite and/or bauxite. The charnockite unit is dominated by pyroxenes + plagioclase + oxides ± garnet. Olivine may be present in minor amounts. Some charnockite outcrops tend to be anorthositic owing to local abundance of plagioclase, gneissic banding is common in charnockites, and leucosomes and melanosomes are generally concentrated along the banding because of migmatization. An amphibole unit, occurring concordantly to the general rock foliation, is located in the northwest corner of the map (see Fig. 1). In addition, lenses of spinel-bearing pyroxenite containing coarse-grained sapphirine occur as disseminations along the khondalite-charnockite contact.

SAMPLES AND PETROGRAPHY

Samples (S25 to S30), hereafter referred to as samples 25, 26, 27, 28, 29, and 30, were selected for detailed

---

* Present address: Applied Geoscience Branch, Whiteshell Nuclear Research Establishment, Pinawa, Manitoba R0E 1L0, Canada.

0003–004X/88/0708–0692$02.00

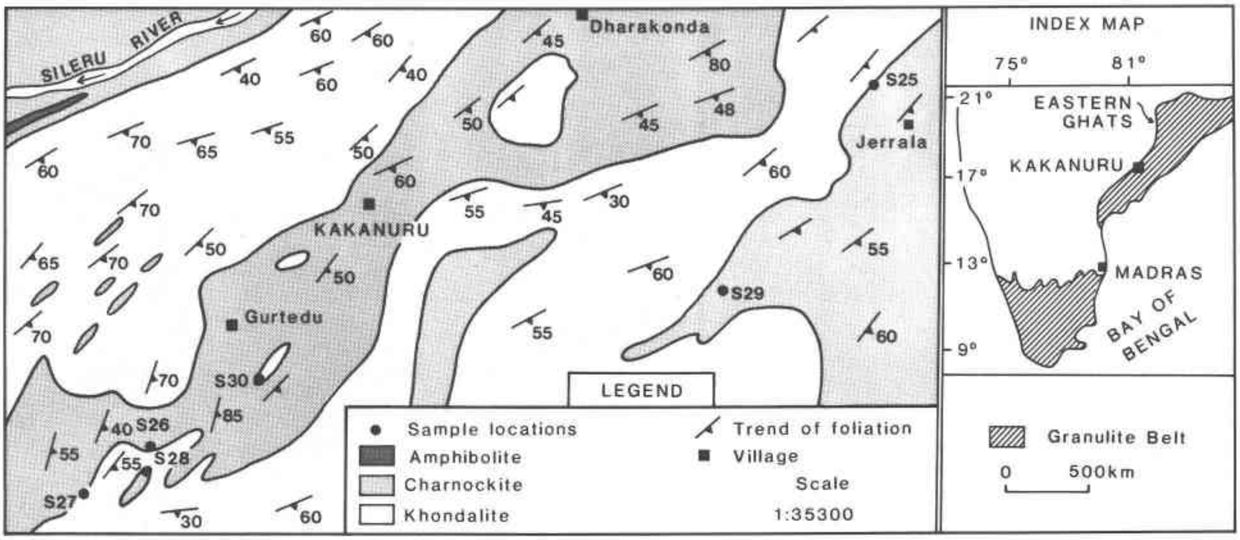

Fig. 1. Geologic map of the Kakanuru area showing locations of samples studied. The location of Kakanuru in the Eastern Ghats is shown in the index map.

petrochemical study. Five of the studied samples are sapphirine-bearing; one was collected at a khondalite-charnockite contact (sample 25), three from pyroxenite lenses (samples 26, 27, and 28), and the fifth from khondalite (sample 30). Sample 29 belongs to the charnockite unit and is devoid of sapphirine. The sample locations and mineral assemblages are shown in Figure 1 and Table 1, respectively.

Sample 25 is essentially composed of sapphirine + magnetite + sillimanite (Fig. 2). Apatite and magnetite are present as inclusions in some sapphirine grains. Fine acicular hematite and/or magnetite are concentrated in cleavages of both sapphirine and sillimanite. A weak preferred orientation is present, and coarse hematite needles cut across the long dimension of sapphirine and sillimanite. The sapphirine grains display light blue to dark blue pleochroism, and some large grains contain small inclusions of sapphirine with the same optical properties but not in optical continuity. Sillimanite prisms are interspersed between large sapphirine grains throughout, and some of them show strain.

Samples 26, 27, and 28 are similar in terms of mineral assemblages and textures. The only distinction is that 26 also contains spinel. All are coarse-grained and characterized by the assemblage sapphirine + orthopyroxene + phlogopite + monazite ± spinel. Zircon and rutile are present in minor amounts. Sapphirine occurs as large grains displaying weak pleochroism from pale blue to colorless. Rodlike inclusions of rutile are common in sapphirine. In sample 26, sapphirine invariably occurs as a

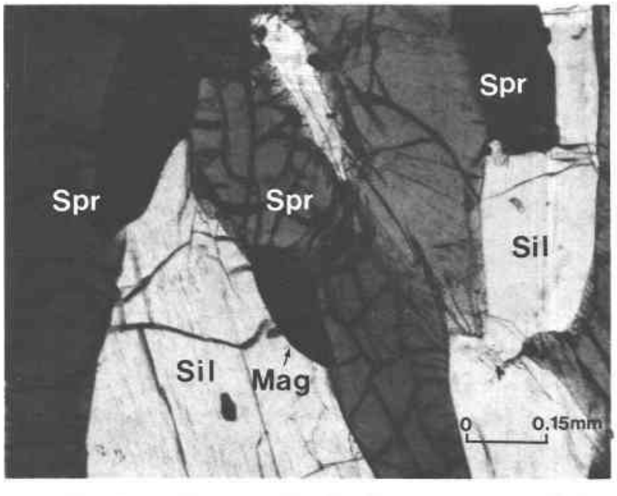

Fig. 2. Photomicrograph showing the assemblage sapphirine (Spr) + sillimanite (Sil) + magnetite (Mag). Sample 25.

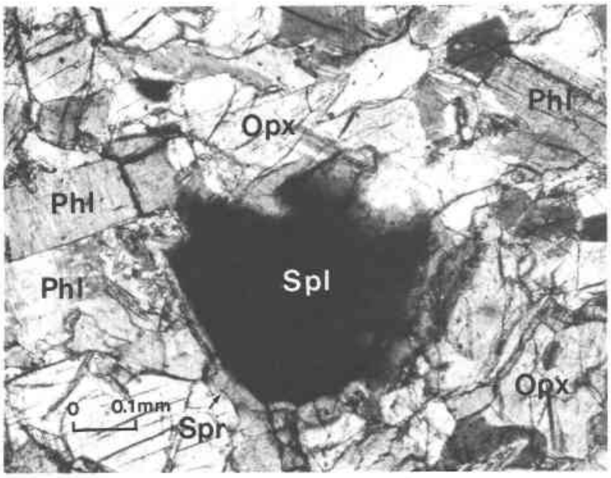

Fig. 3. Photomicrograph of spinel-bearing (Spl) pyroxenite. Note sapphirine (Spr) rim around spinel. Also note phlogopite (Phl) and orthopyroxene (Opx). Sample 26.

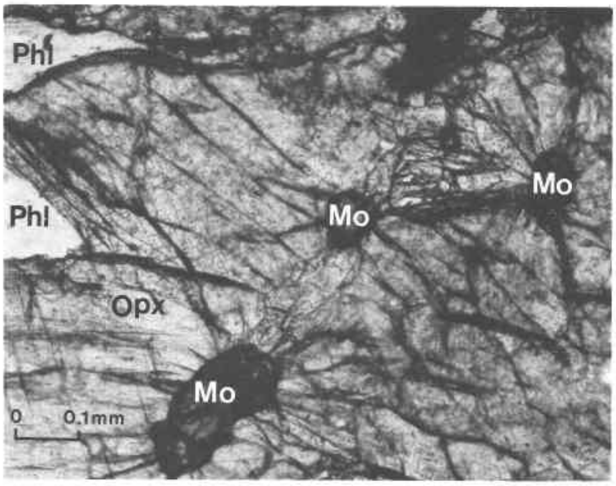

Fig. 4. Photomicrograph showing monazite (Mo), with radial microfractures around, in sapphirine-bearing pyroxenite. Note phlogopite (Phl) and orthopyroxene in the matrix. Sample 28.

thin rim around spinel (Fig. 3). Orthopyroxene shows two well-developed cleavages and weak pleochroism from brown to colorless. A few orthopyroxene and sapphirine grains are fragmented and enclosed in phlogopite prisms, implying that they are early in the paragenesis. Euhedral and some semi-rounded grains of monazite are concentrated as clusters in some domains. Some monazite grains show radial microfractures around them owing to metamictization (Fig. 4).

Sample 29 is a coarse-grained rock with an abundance of plagioclase (see Table 1). The plagioclase grains show residual strain in the form of kinked twin lamellae; some grains show antiperthetic texture. Acicular rutile and spinel inclusions are generally aligned parallel to twin lamellae in plagioclase. Pyroxenes, olivine, and biotite are concentrated around plagioclase boundaries. Spinel grains invariably occur as inclusions in ferromagnesian minerals. Minor alteration, concentrated along grain boundaries and extensional fractures, produced quartz, carbonate, and chlorite.

Sample 30 is a khondalite that has minor amounts of sapphirine (<2%). The most important textural characteristic of this sample is the presence of coronas: (1) sapphirine rims around spinel and magnetite, which in turn are rimmed by garnet, and (2) sillimanite rims around oxides (spinel and magnetite), which in turn are also rimmed by garnet (Fig. 5). Ilmenite lamellae are noted in magnetite in polished sections. Biotite is sporadically distributed throughout in amounts of <1%. Plagioclase is polysynthetically twinned and shows perthitic and mesoperthitic texture. Quartz and sapphirine are present, in direct contact, in one domain.

BULK ROCK AND MINERAL ANALYSES

TABLE 1. Mineral assemblages of samples investigated (amounts in vol%)

Sample:	S25	S26	S27	S28	S29	S30
Quartz	—	—	—	—	—	10–25
Orthoclase	—	—	—	—	—	10–25
Plagioclase	—	—	—	—	10–25	10–25
Olivine	—	—	—	—	1–5	—
Orthopyroxene	—	10–25	10–25	10–25	1–2	—
Clinopyroxene	—	—	—	—	1–5	—
Sapphirine	10–25	10–25	10–25	10–25	—	1–5
Sillimanite	10–25	—	—	—	—	1–5
Mica	—	10–25	10–25	10–25	1–5	1–5
Garnet	—	—	—	—	—	10–25
Ilmenite	1–2	—	—	—	1–2	1–2
Magnetite	1–5	—	—	—	—	1–5
Spinel	—	1–5	—	—	1–5	1–5
Pyrite	—	—	—	—	1–2	—
Monazite	1–2	1–5	1–5	1–5	—	1–2
Apatite	1–2	—	—	—	1–2	1–2
Zircon	1–2	1–2	1–2	1–2	—	1–2
Rutile	1–2	1–2	1–2	1–2	1–2	1–2

Bulk chemical analyses of pulverized rock samples were performed using the ICP method at the Analytical Laboratory of the Geological Survey of Canada. FeO was determined by the wet-chemical method. Rare-earth elements (REEs) were determined by ICP on trace-element solutions that were preconcentrated by a factor of 10 after separation of major elements through ion-exchange resins.

Oxygen-isotope analyses were carried out on an aliquot of bulk rock powder. Oxygen was extracted with BrF_5 and converted to CO_2 prior to spectrometric analysis, as described by Clayton and Mayeda (1963). Isotopic values are reported as $\delta^{18}O$ in per mil relative to standard mean ocean water (SMOW). The results of the bulk rock chemical analyses and oxygen-isotope analyses are listed in Table 2.

Microprobe analyses of silicates and oxides were performed on a MAC electron microprobe, using C-coated polished thin sections. The instrumental conditions were as follows: accelerating potential, 20 kV; specimen current, 10 nA; counting time, 100 s. Natural standards were used for all the minerals analyzed. Sodalite was used for Cl in biotite. The raw data were corrected for background, nonresolution, and matrix effects using the MAGIC V program (Colby, 1980). For each mineral, a number of grains were analyzed to assess the inhomogeneity between grains and also a number of spots within a single grain to investigate possible zonation. As alkali feldspar contains exsolution lamellae, its analyses were reintegrated; magnetite grains and their contained ilmenite lamellae were analyzed separately. Monazites were analyzed on a CAMECA probe using REE II and REE III standards (Drake and Weill, 1972). The mineral analyses are presented in Tables 3 to 8.

BULK ROCK CHEMISTRY

An examination of the chemical composition (Table 2) of the samples studied shows some distinct compositional characteristics. Sample 25 is silica undersaturated, rich in Al_2O_3 with a high Fe_2O_3/FeO ratio (1.42). It contains significant TiO_2 and a large amount of MgO. These characteristics can be related to a protolith of residual mate-

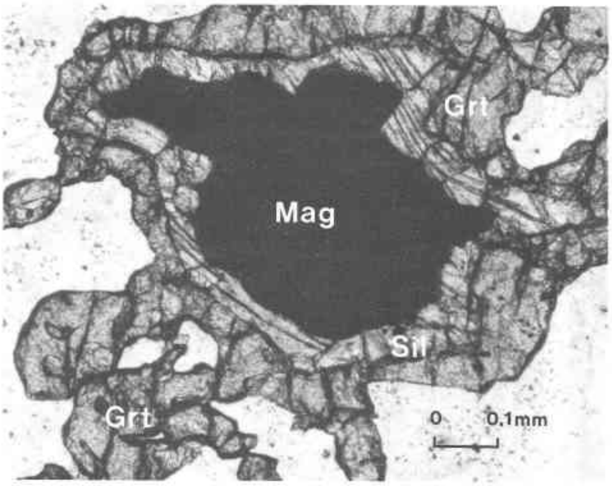

Fig. 5. Photomicrograph of khondalite showing concentric rims of sillimanite (Sil) and garnet (Grt) around magnetite (Mag). Sample 30.

rial such as an aluminous regolith. A similar protolith has been identified by Meng and Moore (1972) for some sapphirine granulites in Labrador, Canada. The chondrite-normalized REE pattern shows depletion of intermediate REEs (see Fig. 6) and is distinct from any of the rock-mineral patterns from continental crust (see Taylor and McClennan, 1985). The pattern represents a composite of the assemblage sapphirine + sillimanite + magnetite.

Samples 26, 27, and 28 have similar chemical characteristics as reflected in their mineralogy. They are low in SiO_2 with large amounts of Al_2O_3 and MgO. The Fe_2O_3/FeO ratio is small (0.38 to 0.51). K_2O is significantly high. They all show steep LREE chondrite-normalized patterns and an enrichment trend of the same from samples 26 to 28 (see Fig. 7). This trend correlates with the increase in monazite and the elimination of spinel.

Compositionally, sample 29 is comparable to the mafic igneous rocks of tholeiitic nature that represent the typical mafic granulite-charnockite suite of the Eastern Ghats. The chondrite-normalized pattern of REEs (Fig. 6) is rather flat, which again is a typical characteristic of tholeiitic rocks. The moderate positive Eu anomaly can be attributed to plagioclase abundance.

Sample 30 is silica saturated and can be considered as a quartzofeldspathic rock of pelitic nature. The chondrite-normalized REE pattern (Fig. 6) shows an abundance of LREEs, a positive Eu anomaly, and a moderate concentration of LREE. High LREEs can be attributed to the presence of the accessary minerals monazite and zircon. Feldspars account for the Eu anomaly, whereas garnet concentrates the HREEs by acting as a sink.

The $\delta^{18}O$ values (Table 2) for all the samples, except 28, are light and range from 4.51 to 6.58‰. Sample 28 has a slightly greater value, 8.40‰. These results compare well with the generally low $\delta^{18}O$ values reported for granulites from the Adirondacks, U.S.A. (Morrison and Valley, 1986), Australia (Allen, 1981; Wilson and Baksi, 1983, 1984), and the Sahara (Fourcade and Javoy, 1973). The $\delta^{18}O$ values, in the present investigation, appear to reflect pregranulite metamorphic signatures, as the values of samples 26 and 27 fall within the range reported for pristine mafic and ultramafic nodules (Kyser, 1986). However, sample 28, belonging to the same category but more affected by metasomatic alteration, has the largest value, suggesting that it is isotopically modified. The $\delta^{18}O$ value of mafic granulite and charnockite (sample 29) falls within the range compiled for mafic igneous rocks (Taylor and Sheppard, 1986). The $\delta^{18}O$ values of samples 25 and 30 probably represent the signatures of their sedimentary protoliths.

TABLE 2. Whole-rock analyses

Sample:	S25	S26	S27	S28	S29	S30
SiO_2 (wt%)	17.16	31.26	41.90	34.30	49.00	69.20
TiO_2	2.35	1.58	1.12	0.80	1.66	1.15
Al_2O_3	55.35	32.71	20.15	30.61	15.20	16.50
Fe_2O_3	7.80	1.50	1.65	1.36	2.20	2.20
FeO	5.50	2.95	4.28	2.83	8.00	4.80
MnO	0.06	0.02	0.03	0.01	0.19	0.10
MgO	11.23	26.60	26.91	25.52	9.22	2.15
CaO	0.02	0.05	0.02	0.07	10.77	0.92
Na_2O	0.00	0.01	0.05	0.00	2.40	0.50
K_2O	0.00	2.50	2.25	2.41	1.04	2.19
H_2O^+	0.11	0.25	0.55	0.72	0.52	0.48
P_2O_5	0.00	0.20	0.16	0.34	0.13	0.03
CO_2	0.00	0.05	0.10	0.10	0.30	0.10
Total	99.58	99.68	99.17	99.07	100.63	100.32
La (ppm)	2.36	122.2	173.4	836.8	7.9	31.8
Ce	4.24	243.5	330.6	1591.0	16.9	50.2
Nd	1.87	98.7	142.8	602.8	11.4	15.3
Sm	0.33	15.6	26.5	58.1	3.29	2.51
Eu	0.05	1.82	2.68	4.98	1.44	1.38
Gd	0.18	15.31	18.36	37.41	4.52	3.41
Tb	0.04	3.42	4.15	8.01	0.67	0.30
Ho	0.15	4.95	6.02	8.78	0.71	0.49
Tm	0.13	2.26	2.53	2.60	0.29	0.25
Yb	0.62	14.80	15.70	18.40	1.89	1.55
Lu	0.11	2.21	2.61	3.05	0.27	0.26
$\delta^{18}O$ (‰)	5.87	4.51	4.96	8.40	6.58	6.41

TABLE 3. Microprobe analyses of sapphirine

Sample:	S25	S26	S27	S28	S30	
					Rim on Fe-Ti oxide	Matrix
SiO_2	14.50	14.85	14.90	14.73	12.49	12.68
Al_2O_3	57.63	61.70	61.27	61.16	60.70	60.32
FeO_t	11.92	3.65	3.22	2.77	10.80	11.48
MnO	0.07	0.00	0.00	0.00	0.00	0.05
MgO	16.47	19.68	20.78	20.97	15.94	15.50
Total	100.59	99.88	100.17	99.63	99.93	100.03
	Number of cations on the basis of 20(O)					
Si	1.711	1.735	1.734	1.721	1.512	1.539
$^{[4]}Al$	4.289	4.265	4.266	4.279	4.488	4.461
$^{[6]}Al$	3.976	4.202	4.142	4.145	4.173	4.135
Fe^{3+}	0.313	0.063	0.124	0.134	0.315	0.326
Fe^{2+}	0.898	0.300	0.189	0.137	0.741	0.746
Mn	0.006	0.000	0.000	0.000	0.000	0.005
Mg	2.915	3.426	3.605	3.651	2.875	2.804
X_{Mg}	0.770	0.919	0.950	0.964	0.795	0.790

TABLE 4. Microprobe analyses of pyroxenes, olivine, and garnet

	Orthopyroxene				Clino-pyroxene	Olivine	Garnet
Sample:	S26	S27	S28	S29	S29	S29	S30
SiO_2	53.32	53.66	54.54	51.05	51.42	34.82	39.37
TiO_2	0.03	0.03	0.04	0.05	0.64	0.02	0.01
Al_2O_3	6.31	5.92	5.53	2.88	5.18	0.35	21.55
FeO_t	8.15	7.23	5.74	21.78	7.51	37.87	24.23
MnO	0.01	0.00	0.02	0.53	0.16	0.55	0.65
MgO	31.95	32.73	34.19	22.92	12.11	26.21	12.52
CaO	0.00	0.00	0.00	0.00	21.49	0.00	1.58
Na_2O	0.00	0.00	0.00	0.31	1.06	0.00	0.00
Total	99.77	99.57	100.06	99.52	99.57	99.82	99.91
	Number of cations on the basis of 6(O) for pyroxenes, 4(O) for olivine, and 24(O) for garnet						
Si	1.857	1.865	1.872	1.910	1.893	0.984	5.982
$^{[4]}Al$	0.143	0.135	0.128	0.090	0.107	0.012	0.018
$^{[6]}Al$	0.116	0.108	0.097	0.035	0.118	0.000	3.842
Ti	0.001	0.001	0.001	0.001	0.180	0.000	0.001
Fe^{3+}	0.026	0.026	0.029	0.073	0.030	0.000	0.000
Fe^{2+}	0.214	0.185	0.133	0.602	0.201	0.895	3.079
Mn	0.000	0.000	0.004	0.011	0.005	0.013	0.084
Mg	1.658	1.695	1.750	1.273	0.719	1.104	2.835
Ca	0.000	0.000	0.000	0.000	0.847	0.000	0.247
Na	0.000	0.000	0.000	0.220	0.076	0.000	0.000
X_{Mg}	0.886	0.902	0.929	0.679	0.781	0.552	0.479

MINERAL CHEMISTRY

Microprobe analyses of various minerals analyzed are given in Tables 3 to 8.

The sapphirine chemistry (Table 3) indicates that there are three populations: (1) an FeO-rich type with relatively lower Al_2O_3 (sample 25), (2) an intermediate type containing moderate amounts of Al_2O_3, FeO, and MgO with lower amounts of SiO_2 (sample 30), and (3) a MgO-rich type with relatively lower FeO (samples 26, 27, and 28). These differences are reflected in X_{Mg} [Mg/(Mg + Fe^{2+})] values, which increase from 0.770 to 0.964 from type 1 to type 3 (see Table 3). Type 2 sapphirine, i.e., sample 30, shows compositional variation in different domains. For example, sapphirine rims around magnetite have higher MgO and lower FeO, compared to sapphirine grains immersed within the quartzofeldspathic matrix. Fe^{3+} calculated according to the method of Higgins et al. (1979) shows values ranging from 0.063 to 0.326 (see Table 3).

The sapphirine compositions, except sample 25, plot (Fig. 8) close to the line defining the common substitution (Mg,Fe,Mn) + Si = 2Al (Deer et al., 1978; Higgins et al., 1979). Deviation of 25 from the common substitution line indicates that it may have been involved in other substitutions as well.

TABLE 5. Microprobe analyses of mica

	Phlogopite				Biotite
Sample:	S26	S27	S28	S30	S29
SiO_2	41.42	42.10	41.08	39.33	35.87
TiO_2	2.85	2.90	3.45	4.14	9.22
Al_2O_3	14.50	13.38	15.07	14.30	13.79
FeO_t	2.68	2.03	2.43	7.68	15.76
MnO	0.00	0.00	0.00	0.04	0.00
MgO	24.21	24.74	23.89	20.72	11.46
CaO	0.05	0.11	0.01	0.07	0.11
Na_2O	0.06	0.52	0.01	0.00	0.05
K_2O	9.82	9.43	10.21	10.04	8.88
Total	95.59	95.21	96.15	96.32	95.14
	Number of cations on the basis of 22(O)				
Si	5.787	5.885	5.715	5.642	5.408
$^{[4]}Al$	2.213	2.115	2.285	2.358	2.451
$^{[6]}Al$	0.175	0.088	0.186	0.060	0.000
Ti	0.299	0.305	0.361	0.446	1.044
Fe^{2+}	0.313	0.238	0.284	0.921	1.985
Mn	0.000	0.000	0.000	0.005	0.000
Mg	5.040	5.152	4.955	4.342	2.570
Ca	0.007	0.017	0.002	0.010	0.018
Na	0.016	0.141	0.000	0.000	0.032
K	1.750	1.681	1.812	1.837	1.705
X_{Mg}	0.941	0.956	0.946	0.825	0.564

Note: S30 contains 0.52% Cl.

TABLE 6. Microprobe analyses of feldspars

	Plagioclase		Orthoclase
Sample:	S29	S30	S30
SiO_2	56.61	58.69	65.32
Al_2O_3	27.61	25.55	18.46
FeO_t	0.13	0.01	0.02
CaO	10.26	8.54	0.62
Na_2O	5.30	6.93	3.81
K_2O	0.42	0.23	12.02
Total	100.33	99.95	100.25
	Number of cations on the basis of 32(O)		
Si	10.147	10.326	11.934
Al	5.832	5.424	3.978
Fe	0.019	0.003	0.003
Ca	1.970	1.648	0.133
Na	1.842	2.420	1.508
K	0.095	0.026	2.558
	Molecular proportions (%)		
Ab	47.14	58.89	35.91
An	50.45	40.43	3.18
Or	2.41	0.62	60.91

TABLE 7. Microprobe analyses of oxides

	Spinel			Magnetite		Ilmenite		
Sample:	S26	S29	S30	S25	S30	S25	S29	S30
TiO_2	0.72	0.11	0.02	15.86	16.04	48.30	47.34	50.20
Al_2O_3	61.55	57.41	59.96	0.40	0.20	0.00	0.00	0.00
Cr_2O_3	0.49	0.36	0.73	0.24	0.11	0.00	0.00	0.00
FeO_t	22.11	32.86	25.95	82.95	83.65	49.75	50.63	48.02
MnO	0.03	0.23	0.02	0.04	0.00	0.16	0.08	0.04
MgO	15.27	8.57	12.94	0.61	0.46	2.05	1.82	2.13
Total	100.17	99.54	99.62	100.10	100.46	100.26	99.87	100.39
	Number of cations on the basis of 4(O) for spinel and magnetite and 3(O) for ilmenite							
Ti	0.014	0.002	0.000	0.448	0.452	0.928	0.913	0.952
Al	1.909	1.899	1.911	0.140	0.072	0.000	0.000	0.000
Cr	0.010	0.008	0.015	0.056	0.022	0.000	0.000	0.000
Fe^{3+}	0.048	0.114	0.084	1.069	1.148	0.125	0.114	0.122
Fe^{2+}	0.447	0.653	0.503	1.406	1.422	0.937	0.965	0.900
Mn	0.000	0.005	0.000	0.001	0.000	0.004	0.002	0.001
Mg	0.599	0.463	0.521	0.042	0.033	0.078	0.070	0.080

Orthopyroxenes, in general, show high X_{Mg} values (up to 0.93), except those in sample 29, which have a lower value (0.68). The high-magnesian nature of the orthopyroxenes categorizes them as enstatite. However, the Al_2O_3 content is quite high for a typical enstatite. Clinopyroxene is augite in composition, which is a typical mineral in mafic charnockites. On the basis of the method of Hamm and Vieten (1971), the pyroxenes show very little Fe^{3+}. Olivine contains significant amounts of FeO as reflected in its intermediate X_{Mg} value (0.55).

Based on X_{Mg} ratios, the mica analyses (Table 5) show two populations: (1) mica from the sapphirine-bearing rocks invariably has high X_{Mg} ratios (0.82 to 0.96) and is termed phlogopite and (2) mica from sample 29 has a lower X_{Mg} value (0.56) and is termed biotite. The biotite is exceptionally rich in TiO_2 and is the most titaniferous one known to the authors. The phlogopites contain relatively high SiO_2 and moderate TiO_2. But phlogopite from sample 30 shows compositional characteristics typical of that mineral from many sapphirine-bearing rocks (see Kamineni and Rao, 1988, and references therein).

Plagioclase feldspar, present in two samples (29 and 30), has anorthite contents in the intermediate range (An_{40} and An_{50}); no chemical zoning is present. Orthoclase contains significant amounts of Na_2O.

Spinels are essentially unzoned and dominated by the spinel-hercynite solid solution, with little Cr_2O_3. Compared to the composition of spinel in charnockite, the spinel in sapphirine granulites has more MgO and Al_2O_3 and less FeO. Calculation of Fe^{3+} following the procedure of Bohlen and Essene (1977) shows significant amounts of Fe^{3+}. Magnetite contains large amounts of TiO_2 and can be termed titanomagnetite. The ilmenite lamellae contain relatively more MgO than the host magnetite.

Monazite shows two compositional trends that can be related to its paragenesis. The monazite grains in the assemblage sapphirine + enstatite + phlogopite are uraniferous and contain greater amounts of SiO_2. On the other

TABLE 8. Microprobe analyses of monazite

Sample	S27	S28	S30
La_2O_3	12.11	12.75	13.48
Ce_2O_3	24.47	25.11	26.22
Pr_2O_3	3.57	3.83	3.75
Nd_2O_3	11.06	11.21	10.18
Sm_2O_3	2.08	2.18	1.86
Gd_2O_3	3.62	3.60	3.32
Dy_2O_3	0.86	0.80	0.64
Er_2O_3	0.19	0.13	0.08
Y_2O_3	3.93	3.64	3.24
ThO_2	9.03	7.71	6.31
UO_2	0.41	0.55	0.00
CaO	0.03	0.05	1.08
P_2O_5	25.14	24.74	27.06
SiO_2	2.46	2.87	1.09
Total	98.96	99.17	98.31

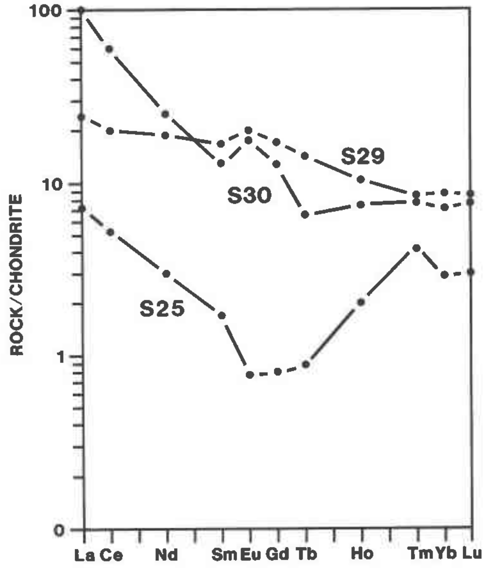

Fig. 6. Chondrite-normalized patterns of REEs for samples 25, 29, and 30. REE data normalized using the chondrite values of Haskin et al. (1968) and Masuda et al. (1973).

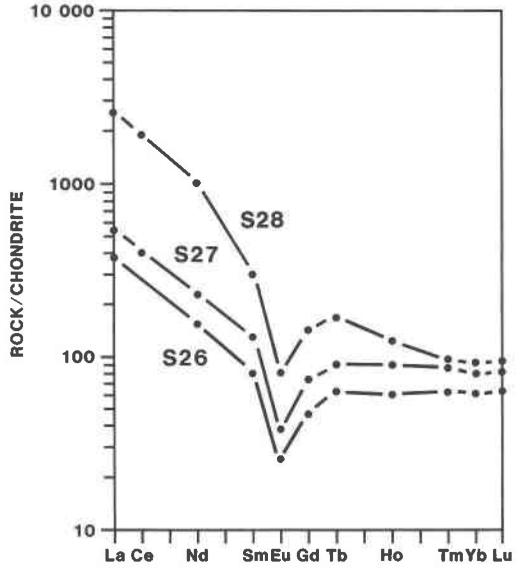

Fig. 7. Chondrite-normalized patterns of REEs for samples 26, 27, and 28. REE data normalized as in Fig. 6.

hand, monazite grains in khondalite are devoid of U and contain greater amounts of CaO. These characteristics may suggest the substitution $Si^{4+} + U^{4+} = 4Ca^{2+}$.

P-T ESTIMATE

Pressure-temperature conditions of metamorphism are estimated, wherever possible, using calibrated geothermometers and geobarometers. Sample 30 provides temperature estimates from the two-feldspar and garnet-biotite geothermometers, whereas sample 29 yields a temperature estimate from the two-pyroxene geothermometer. Pressure is also estimated, in sample 30, on the basis of the plagioclase-garnet-sillimanite-quartz geobarometer. The results are listed in Table 9.

Sample 30 records extremely high temperatures (>1000 °C) from two-feldspar thermometry, regardless of whether binary or ternary solutions are adopted in the estimate.

TABLE 9. Temperature-pressure estimates

Sample	Temperature (°C)	Pressure (kbar)	Reference
			Two-pyroxene geothermometer
29	847		Wood and Banno (1973)
	836		Wells (1977)
	940		Kretz (1982)
			Two-feldspar geothermometer
	1063		Whitney and Stormer (1977)
	1040		Mora and Valley (1985)
			Garnet-biotite geothermometer
30	585		Thompson (1976)
	592		Ferry and Spear (1978)
	595		Perchuk et al. (1981)
			Garnet-sillimanite-plagioclase-quartz geobarometer
		7.3	Newton and Haselton (1981)

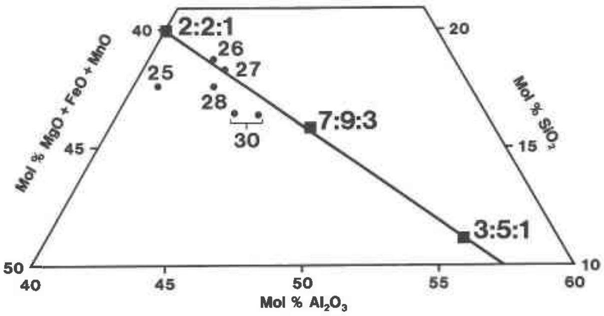

Fig. 8. Composition of sapphirine from the Kakanuru area, projected in the system (MgO + FeO + MnO)-Al_2O_3-SiO_2.

On the other hand, the garnet-biotite geothermometer from the same sample gives moderate temperatures (≃600 °C). This discrepancy can possibly be attributed to a later rehydration event, at lower temperature, that stabilized phlogopite.

The estimated temperature, based on feldspar thermometry, probably represents the maximum for sapphirine granulites in the Kakanuru area. A minimum temperature, however, can be inferred from coexisting sapphirine + quartz as they are stable together only at, or in excess of, 6 kbar and 850 °C (Grew, 1982). Similar conditions have also been deduced for the sapphirine + quartz occurrence, near Vizianagaram town, located in the eastern part of the Eastern Ghats (Kamineni and Rao, 1988). Much higher temperature estimates are reported for sapphirine + quartz from Antarctica: 900 °C (Grew, 1980), 950 °C (Harley, 1985), 980 °C (Ellis et al., 1980), and >1000 °C (Sandiford and Powell, 1986).

The pyroxene thermometry (from sample 29) yields temperatures between 836 and 940 °C, suggesting that the minimum temperature assigned for sample 30 is not unrealistic.

The pressure estimate, i.e., 7.3 kbar, for sample 30 is conformable with the temperature estimates. The *P-T* conditions, in general, are analogous to those of sapphirine granulites reported from Enderby Land (Grew, 1980). Development of mesoperthitic textures in K-feldspar is also compatible with the extremely high grade nature of metamorphism.

PARAGENESES OF SAPPHIRINE

Sapphirine-bearing rocks of various parageneses were reported from the Precambrian terrane of India, the southern region in particular. Generally, sapphirine occurs in metasedimentary rocks containing the assemblage garnet + sillimanite + orthopyroxene + cordierite and in pyroxene granulites in the charnockite region of south India (Grew, 1982).

Walker and Collins (1907) described sapphirine as a reaction product between spinel-bearing ultramafic magma and sillimanite-bearing aluminous rock in the Madugula area of the Eastern Ghats. Rao (1971) also supported a similar origin for a sapphirine occurrence in bronzite pyroxenites from the Anakapalli area. In addition, sapphirine is also reported from reaction zones between chromite-rich ultramafic layers and anorthosite in the Sittampundi complex (Janardhan and Leake, 1974) and in ultramafic enclaves in amphibolites of southern Karnataka (Janardhan and Shadakshara Swamy, 1982).

In the Kakanuru area, the three types of sapphirine distinguished by us on the basis of associated minerals and chemistry have distinct parageneses. Type 1 sapphirine (sample 25), the most Fe-rich variety, is associated with sillimanite and iron oxides. The bulk composition of the host rock can be approximated as SiO_2-Al_2O_3-Fe_2O_3-FeO-MgO, with TiO_2 being an additional component. Presumably, the silica-undersaturated character combined with high Al_2O_3 and MgO provided chemical conditions conducive for sapphirine development. The high Fe_2O_3/FeO ratio (1.42) indicates that the sapphirine-forming reactions were oxidative.

Type 2 sapphirine (in sample 30) shows textures that are useful to deduce reactions responsible for its formation. Sapphirine rims around spinel indicate that the latter was a definite reactant in the formation of the former. Since quartz is present, but always shielded from spinel by sapphirine, the following reaction can be suggested:

$$\underset{\text{Spinel}}{2(MgFe)Al_2O_4} + \underset{\text{Quartz}}{SiO_2} = \underset{\text{Sapphirine}}{(MgFe)_2Al_4SiO_{10}}. \qquad (1)$$

In addition, the rims of sapphirine around magnetite indicate that iron oxides were also involved, and the reaction was of an oxidative type as evidenced by significant Fe^{3+} in sapphirine. Rims of garnet around sapphirine suggest that it subsequently reacted to produce that phase.

Type 3 sapphirine, occurring in samples 26, 27, and 28, is analogous to "enstatite type" paragenesis from Greenland, described by Herd et al. (1969). The "enstatite type" contains the assemblage sapphirine + enstatite + spinel + phlogopite ± pargasite, which is almost identical to sample 26 of the present study. Herd et al. (1969) identified a Mg- and Al-rich spinel-bearing ultramafic rock as a protolith for a sapphirine-bearing assemblage. According to these authors, the ultramafic rock had been metasomatized and replaced by sapphirine and other minerals. This appears to be true in the case of type 3 sapphirine as well. Originally, samples 26, 27, and 28 were spinel-bearing pyroxenites, later modified profoundly by metasomatism. The most profound effects of metasomatism are the growths of phlogopite and monazite due to addition of K, LREEs, actinides (U and Th), and H_2O. Sapphirine growth, however, appears to have preceded the onset of K metasomatism, as it is commonly enclosed in biotite prisms. Rims of sapphirine around spinel and concentrations of rutile needles in sapphirine support the interpretation that sapphirine grew at the expense of spinel; the rutile needles can be interpreted to have formed from liberation of TiO_2, present in spinel, which was not accommodated in the sapphirine. Evidently, SiO_2 must have been added to promote sapphirine growth, as indicated in Reaction 1. The source of silica could be either external, introduced by metasomatism, or internal, released because of formation of other minerals such as phlogopite. But the textural evidence mitigates against the latter possibility. The preferential replacment of spinel by sapphirine at pyroxenite-khondalite contacts provides evidence for addition of silica from the khondalite. Considering the steep chemical gradients between undersaturated pyroxenite and saturated khondalite, this process appears highly likely to have occurred. Subsequently, the spinel + sapphirine pyroxenites were affected by metasomatism resulting in growth of phlogopite and monazite. The source of elements involved in metasomatism can be linked to younger granitic intrusions in the Eastern Ghats. Plutonic activity, during late Proterozoic time, comprising granitic bodies as a major component, is well recognized in the Eastern Ghats covering parts of northeastern Andhra Pradesh and southern Orissa provinces (Halden et al., 1982; Perraju et al., 1979). The present study area falls within these regions.

CONCLUDING REMARKS

The granulite metamorphic belt of the Eastern Ghats around Kakanuru contains sapphirine occurrences that have three types of parageneses as well as compositional characteristics. Type 1 and type 2 sapphirines formed isochemically in rocks of suitable bulk composition under extremely high temperatures ranging from 850 to 1000 °C. Type 3 sapphirine also formed at the same time by replacing spinel in pyroxenite lenses that are concentrated along charnockite-khondalite contacts. This process requires addition of silica, which is interpreted to have been supplied by khondalite occurring in the immediate vicinity.

Some of the sapphirine granulites were affected subsequently by metasomatism that produced phlogopite and monazite. The metasomatic effects are well pronounced in type 3 sapphirine-bearing rocks, possibly because of their location. The charnockite-khondalite contact along which type 3 sapphirine granulites are concentrated may have acted as the most favorable pathway for migration of matter during the metasomatic event. The source of the constituents involved in metasomatism, namely K, LREEs, and actinides (U and Th), is linked to the granitic plutonic activity that was prevalent in the Eastern Ghats during late Proterozoic time.

ACKNOWLEDGMENTS

We sincerely thank P. F. Augustine, Geological Survey of India, for helpful discussions and Maurizio Bonardi, Geological Survey of Canada, for providing microprobe facilities. Robert Kerrich, University of Saskatchewan, kindly carried out the oxygen-isotope analysis. Critical comments by two referees helped to improve the quality of the paper. We also thank Dr. J. Alex Speer, North Carolina University, for encouragement to revise the paper. Pat Lucas patiently typed the manuscript.

REFERENCES CITED

Ackermand, D., Seifert, F., and Schreyer, W. (1975) Instability of sapphirine at high pressures. Contributions to Mineralogy and Petrology, 50, 79–92.

Allen, A.R. (1981) Origin of hydrous cordierite and isotopically light oxygen in granulite facies rocks, Strangways Range, central Australia. Mineralogical Magazine, 44, 63–68.

Bishop, F.C., and Newton, R.C. (1975) The composition of low pressure synthetic sapphirine. Journal of Geology, 83, 511–517.

Bohlen, S.R., and Essene, E.J. (1977) Feldspar and oxide thermometry of granulites in the Adirondacks Highlands. Contributions to Mineralogy and Petrology, 62, 153–169.

Clayton, R.N., and Mayeda, T.K. (1963) The use of bromine pentafluoride in the extraction of oxygen from oxides and silicates. Geochimica et Cosmochimica Acta, 27, 43–52.

Colby, J.W. (1980) MAGIC V—A computer program for quantitative electron-excited energy-dispersive analysis. Instruction manual QUANTEX RAY$^{\text{th}}$, Appendix E, ED-1: 1/8/80, Kevex Corporation, Foster City, California.

Deer, W.A., Howie, R.A., and Zussman, J. (1978) Rock-forming minerals, vol. 2A, Single-chain silicates (2nd edition). Wiley, New York.

Drake, M.J., and Weill, E.F. (1972) New rare earth element standards for electron microprobe analysis. Chemical Geology, 10, 179–181.

Ellis, D.J., Sheraton, J.W., England, R.N., and Dallwitz, W.B. (1980) Osumilite-sapphirine-quartz granulites from Enderby Land, Antarctica—Mineral assemblages and reactions. Contributions to Mineralogy and Petrology, 72, 123–143.

Ferry, J.M., and Spear, F.S. (1978) Experimental calibration of the partitioning of Fe and Mg between biotite and garnet. Contributions to Mineralogy and Petrology, 66, 113–116.

Fourcade, S., and Javoy, M. (1973) Rapports $^{18}O/^{16}O$ dans les roches du vieux socle catazonal d'In Ouzzel (Sahara algérien). Contributions to Mineralogy and Petrology, 42, 235–242.

Grew, E.S. (1980) Sapphirine + quartz association from Archean rocks of Enderby Land, Antarctica. American Mineralogist, 65, 821–836.

——— (1982) Sapphirine, kornerupine, and sillimanite + orthopyroxene in the charnockite region of south India. Journal of Geological Society of India, 10, 469–505.

Halden, N.M., Bowes, D.R., and Dash, B. (1982) Structural evolution of migmatites in granulite facies terrane: Precambrian crystalline complex of Angul, Orissa, India. Transactions of the Royal Society of Edinburgh, Earth Sciences, 73, 109–118.

Hamm, H.M., and Vieten, K. (1971) Zur Berechnung der Kristallochemichen Formel und des Fe^{3+} gehlites von klinopyroxen electrostrahlimikroanalysen. Neues Jahrbuch für Mineralogie Monatshafte, 310–314.

Harley, S.L. (1985) Garnet-orthopyroxene bearing granulites from Enderby Land, Antarctica: Metamorphic pressure-temperature-time evolution of the Archean Napier Complex. Journal of Petrology, 26, 819–856.

Haskin, L.A., Haskin, M.A., and Frey, F.A. (1968) Relative and absolute abundances of rare earths. In L.H. Ahrens, Ed., Origin and distribution of elements, p. 889–912. Pergamon, Oxford.

Hensen, B.J. (1986) Theoretical phase relations involving cordierite and garnet revisited: The influence of oxygen fugacity on the stability of sapphirine and spinel in the system Mg-Fe-Al-Si-O. Contributions to Mineralogy and Petrology, 92, 362–367.

——— (1987) *P-T* grids for undersaturated granulites in the system MAS ($n + 4$) and FMAS ($n + 3$)—Tools for the derivation of *P-T* paths of metamorphism. Journal of Metamorphic Geology, 5, 255–271.

Herd, R.K., Windley, B.F., and Ghisler, M. (1969) The mode of occurrence and petrogenesis of the sapphirine-bearing and associated rocks of West Greenland. Geological Survey of Greenland Report 24, 44 p.

Higgins, J.B., Ribbe, P.H., and Herd, R.K. (1979) Sapphirine I: Crystal chemical contributions. Contributions to Mineralogy and Petrology, 68, 349–356.

Janardhan, A.S., and Leake, B.E. (1974) Sapphirine in the Sittampundi complex, India. Mineralogical Magazine, 39, 901–902.

Janardhan, A.S., and Shadakshara Swamy, K. (1982) A preliminary report on the occurrence of sapphirine in the ultramafic enclave near Terakanambi, southern Karnataka. Current Science, 51, 43–44.

Kamineni, D.C., and Rao, A.T. (1988) Sapphirine-bearing quartzite from the Eastern Ghats granulite terrain, Vizianagarum, India. Journal of Geology, 96, 209–220.

Kretz, R. (1982) Transfer and exchange equilibria in a portion of the pyroxene quadrilateral as deduced from natural and experimental data. Geochimica et Cosmochimica Acta, 46, 411–421.

Kyser, T.K. (1986) Stable isotope variations in the mantle. Mineralogical Society of America Reviews in Mineralogy, 16, 141–162.

Masuda, A., Nakumura, N., and Tanaka, T. (1973) Fine structure and mutually normalized rare-earth patterns of chondrites. Geochimica et Cosmochimica Acta, 37, 239–248.

Meng, L.K., and Moore, J.M., Jr. (1972) Sapphirine-bearing rocks, Wilson Lake, Labrador. Canadian Mineralogist, 11, 779–790.

Mora, C.I., and Valley, J.A. (1985) Ternary feldspar thermometry in granulites from the Oaxacan Complex, Mexico. Contributions to Mineralogy and Petrology, 89, 215–225.

Morrison, J., and Valley, J.A. (1986) Pre-metamorphic magmatic contamination of Marcy anorthosite massif, Adirondack Mountains, N.Y. Terra Cognita, 6, no. 2, 209–218.

Newton, R.C. (1972) An experimental determination of the pressure stability limits of magnesian cordierite under wet and dry conditions. Journal of Geology, 80, 398–420.

Newton, R.C., and Haselton, H.T. (1981) Thermodynamics of the garnet-plagioclase-Al_2SiO_5-quartz geobarometer. In R.C. Newton, A. Navrotsky, and B.J. Wood, Eds., Thermodynamics of minerals and melts, p. 131–147. Springer-Verlag, New York.

Perchuk, L.L., Podlesskii, K.K., and Aranovich, L. Ya. (1981) Calculation of thermodynamic properties of end-member minerals from natural paragenesis. In R.C. Newton, A. Navrotsky, and B.J. Wood, Eds., Thermodynamics of minerals and melts, p. 111–130. Springer-Verlag, New York.

Perraju, P., Kovach, A., and Svinger, E. (1979) Rubidium-strontium ages of some rocks from parts of the Eastern Ghats in Orissa and Andhra Pradesh, India. Journal of Geological Society of India, 20, 290–296.

Rao, K.S.R. (1971) Mineralogy and petrology of charnockitic and associated rocks of Anakapalli area, Visakhapatnam District, Andhra Pradesh, India. Ph.D. thesis, Andhra University, 308 p.

Sandiford, M., and Powell, R. (1986) Pyroxene exsolution in granulites from Fyfe Hills, Enderby Land, Antarctica: Evidence for 1000°C metamorphic temperatures in Archean continental crust. American Mineralogist, 71, 946–954.

Seifert, F. (1974) Stability of sapphirine: A study of the aluminous part of the system MgO-Al_2O_3-SiO_2-H_2O. Journal of Geology, 82, 173–204.

Singh, K., and Augustine, P.F. (1978) Sapphirine-bearing rocks in parts of the Eastern Ghats and their significance. Indian Minerals, 32, 48–50.

Taylor, H.P., Jr., and Sheppard, S.M.F. (1986) Igneous rocks: I. Processes of isotopic fractionation and isotopic systematics. Mineralogical Society of America Reviews in Mineralogy, 16, 227–269.

Taylor, S.R., and McClennan, S.M. (1985) The continental crust: Its composition and evolution, 318 p. Blackwell Scientific Publications, Oxford.

Thompson, A.B. (1976) Mineral reactions in pelitic rocks: II. Calculations of some *P-T-X* (Fe-Mg) phase relations. American Journal of Science, 276, 425–454.

Walker, T.L., and Collins, W.H. (1907) Petrological study of some rocks from the hill tracts, Visakhapatnam District, Madras Presidency. Geological Survey of India Records, 36, 1–18.

Wells, P.R.A. (1977) Pyroxene thermometry in simple and complex systems. Contributions to Mineralogy and Petrology, 62, 129–139.

Whitney, J.A., and Stormer, J.C., Jr. (1977) The distribution of $NaAlSi_3O_8$ between coexisting microcline and plagioclase and its effect on geothermometric calculations. American Mineralogist, 62, 687–691.

Wilson, A.F., and Baksi, A.K. (1983) Widespread ^{18}O depletion in some Precambrian granulites of Australia. Precambrian Research, 23, 33–56.

——— (1984) Oxygen isotope fractionation and disequilibrium displayed by some granulite facies rocks from Fraser Range, Western Australia. Geochimica et Cosmochimica Acta, 48, 423–432.

Wood, B.J., and Banno, S. (1973) Garnet-orthopyroxene and orthopyroxene-clinopyroxene relations in simple and complex systems. Contributions to Mineralogy and Petrology, 42, 109–124.

MANUSCRIPT RECEIVED OCTOBER 21, 1986
MANUSCRIPT ACCEPTED MARCH 4, 1988